DE-FE0031709 Novel Modular Electrocatalytic Processing for Simultaneous Conversion of Carbon Dioxide and Wet Shale Gas into Valuable Products

Jason Trembly, PhD

August 31, 2021

2021 CARBON MANAGEMENT AND OIL AND GASRESEARCH PROJECT REVIEW MEETING

Create for Good.

RUSS COLLEGE OF ENGINEERING AND TECHNOLOGY

OHIO UNIVERSITY

Disclaimer

"This report was prepared as an account of work sponsored by an agency of the United States Government. Neither the United States Government nor any agency thereof, nor any of their employees, makes any warranty, express or implied, or assumes any legal liability or responsibility for the accuracy, completeness, or usefulness of any information, apparatus, product, or process disclosed, or represents that its use would not infringe privately owned rights. Reference herein to any specific commercial product, process, or service by trade name, trademark, manufacturer, or otherwise does not necessarily constitute or imply its endorsement, recommendation, or favoring by the United States Government or any agency thereof. The views and opinions of authors expressed herein do not necessarily state or reflect those of the United States Government or any agency thereof."

Commercial CO Production

- Industrial bulk CO is produced by separating CO from syngas (containing H_2) generated via steam methane reforming (SMR) using natural gas as the feedstock.

- Various separation technologies are used including cryogenic separation (i.e. cold box), pressure swing adsorption (PSA), membrane separation, and ammonium salt solution absorption.

- The compression/expansion and high degree of heat integration required for this process make it capital intensive with CO pricing sensitive to process scale.

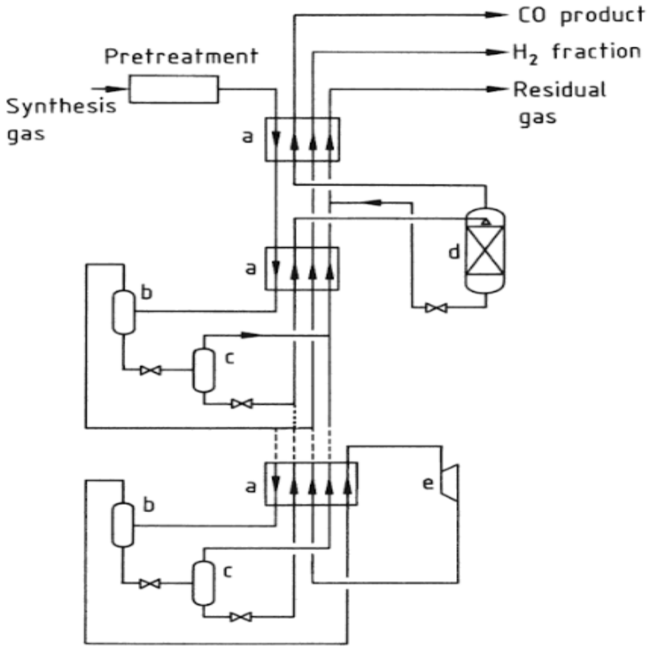

Figure 1. Bulk CO Production Using Cryogenic Partial Condensation Process.

U.S. Natural Gas Liquids (NGLs) Supply

- U.S. Unconventional Resources
  - Tremendous growth of NGL supply
- NGL Processing & Management
  - C_{2+} alkanes separated by turbo-expansion and cryogenic distillation
  - Ethane rejection, reinjection, exportation
- Associated Issues
  - Insufficient infrastructure linking NGL sources to consumers
  - Prime value hydrocarbons sold for fuel value
  - Unrealized economic value of petrochemical supply-chain

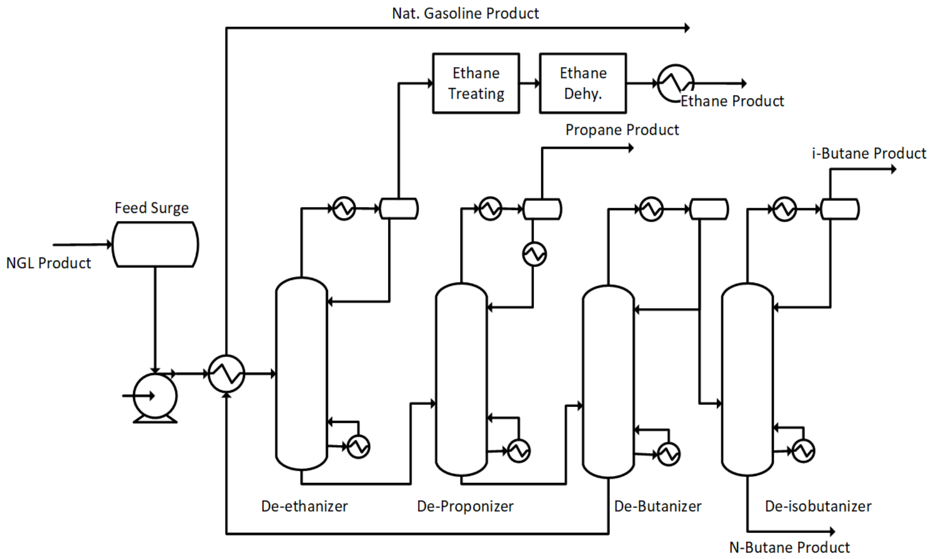

Figure 2. Current U.S. Ethane Production and Conversion Capacities [1].

Figure 3. Turbo-expander process for C_{2+} separation

Figure 4. NGL fractionation train

1. Petrochemical Update (2016, March). US Ethane and Ethylene Exports & Market Report.

Background: SOEC for CO_2 and WNG Conversion

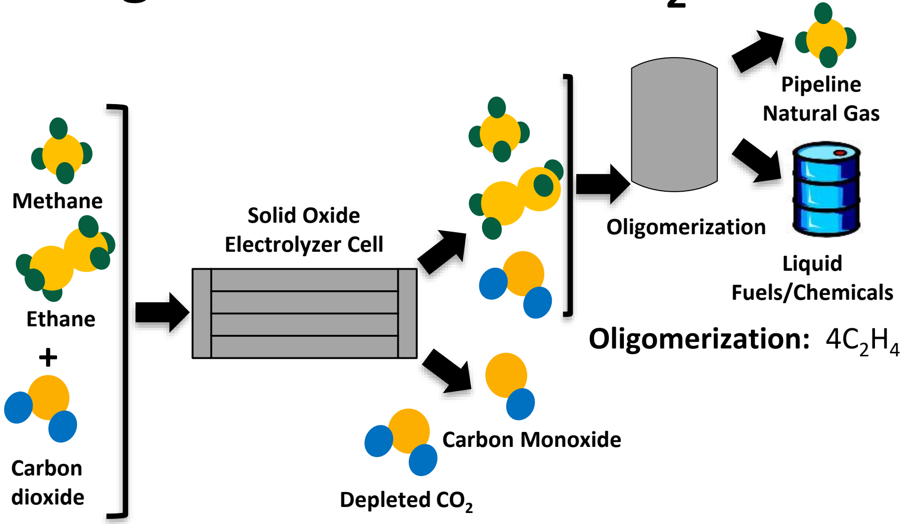

Oligomerization: $4C_2H_4 \rightarrow C_8H_{16}$

Cathode 1: $CO_2+2e^- \rightarrow CO+O^{2-}$ Eq. 1

Anode: $C_2H_6+O^{2-} \rightarrow C_2H_4+H_2O+2e^-$ Eq. 2

Overall 1: $C_2H_6+CO_2 \rightarrow CO+C_2H_4+H_2O$; $E_{700°C}$: -0.09V Eq. 3

Cathode 2: $O_2+4e^- \rightarrow 2O^{2-}$ Eq. 4

Anode: $C_2H_6+O^{2-} \rightarrow C_2H_4+H_2O+2e^-$ Eq. 5

Overall 2: $C_2H_6+0.5O_2 \rightarrow C_2H_4+H_2O$; $E_{700°C}$: +0.94V Eq. 6

Proce

- Ut m
  - –
  - – s
  - –
  - – , or eld
- Pr CO ar ec
- Lo
- Ac bottleneck facing the U.S. natural gas industry

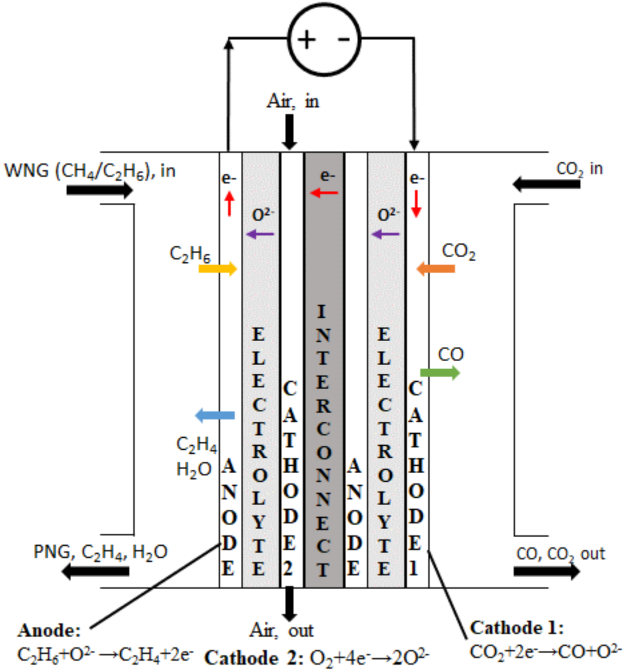

Figure 4: SOEC for simultaneous conversion CO_2/WNG conversion

Project Objectives

- Simultaneous conversion of CO_2 and NGLs (C_2H_6) in wet natural gas (WNG) into valuable CO and chemicals/fuels respectively, using electrical energy

- Primary - Identify an intermediate temperature solid oxide electrolyzer cell (SOEC) process configuration for producing CO and removing C_2H_6 from WNG
  - Costs equivalent to current commercial processes
  - Significant reduction in lifecycle CO_2 emissions over conventional processes

- Secondary - Potential integration of the proposed process into a coal-fired power plant facility for direct utilization of CO_2 containing flue gas to match current commercial CO production and NGL separation costs

Catalyst Infiltration

Precursor solution

- Volume: 25 ml
- Metal concentration: 1M
- Triton X-100 (surfactant): 19.2 mM
- Ethanol to water volume ratio: 1:1
- Citric acid (alloy infiltration only): 0.2 M

Infiltration technique

- Transferring precursor solution into the porous scaffold using micro pipette
- Using vacuum system
- Repeating first two steps four times
- Drying cells on a hot plate at an intermediate temperature (120 ˚C)
- Decomposing nitrates at high temperature (450 ˚C) using a hot plate
- Repeating infiltration steps until desired weight loading is achieved (35wt% of cathode)

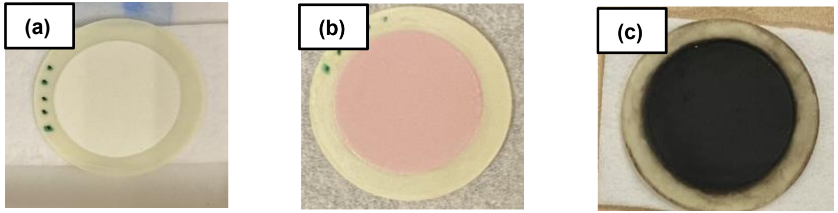

Figure 2. Cobalt infiltrated GDC scaffold electrode at different stages of infiltration: (a) before infiltration, (b) after first infiltration cycle (c) after final sintering at 900 °C for 3 hours.

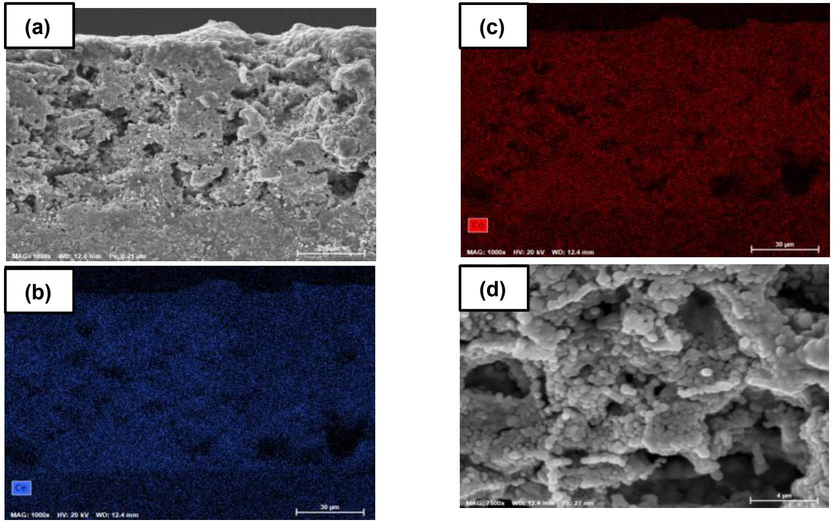

Figure 5. Cross sectional SEM images of cobalt infiltrated GDC scaffold: (a) cell cross section, (b) cerium distribution representing the GDC scaffold , (c) cobalt distribution throughout the scaffold, and (d) zoomed-in view inside scaffold structure.

Transition Metals Electrochemical Performance (850 ℃)

81%CO2-10%CO-9%N2 gas composition was used during tests

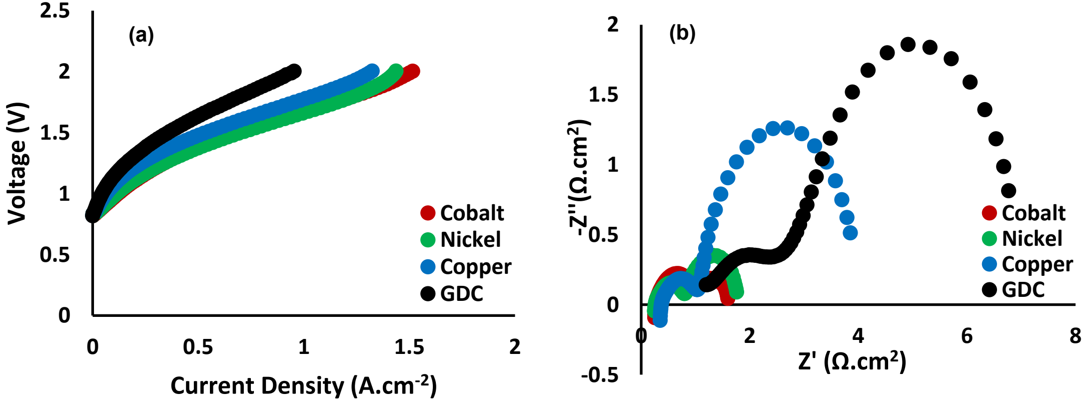

Figure 6. Performance of different transition metal infiltrated cathodes tested at 850℃ : (a) polarization curves and (b) Nyquist curves.

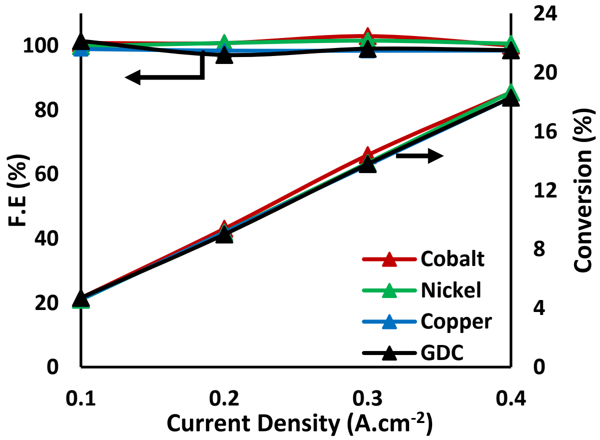

Figure 7. Faradaic efficiency and CO_2 conversion for transition metal infiltrated cathodes tested at 850℃.

Long Term CO_2 electrolysis Test (Cobalt infiltrated cell)

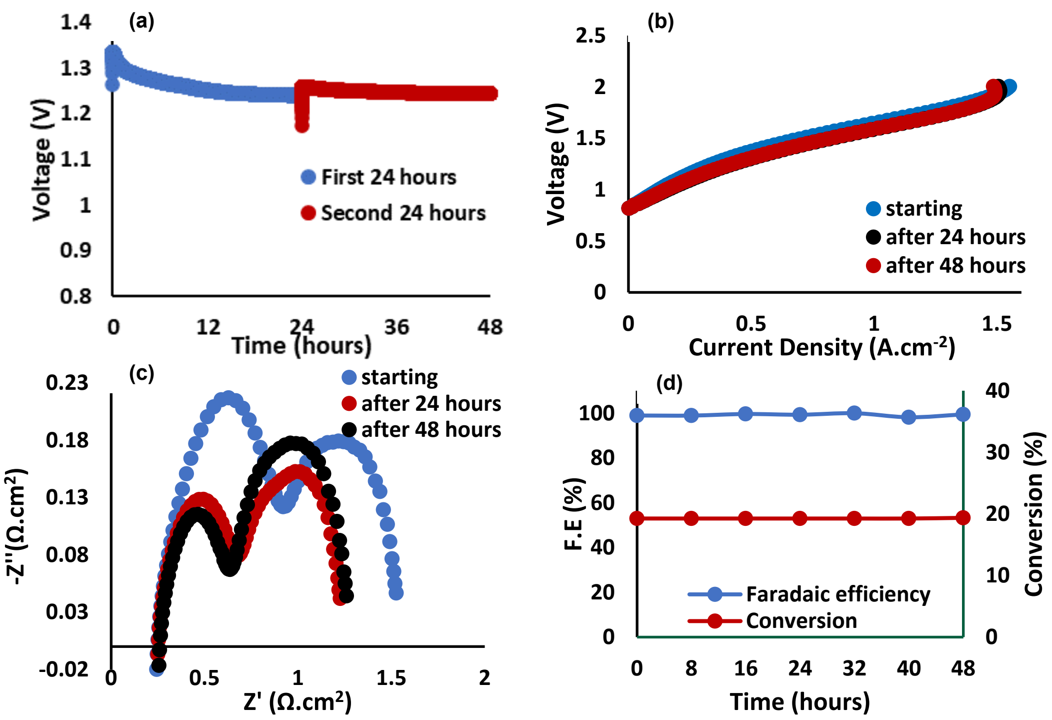

Figure 8. Long term CO_2 electroreduction performance of cobalt infiltrated cathodes at 850°C: (a) Galvanostatic test at 0.4 A.cm^{-2} for 48 hours, (b) Polarization curves, (c) Nyquist plots, and (d) Faradaic efficiency and CO_2 conversion

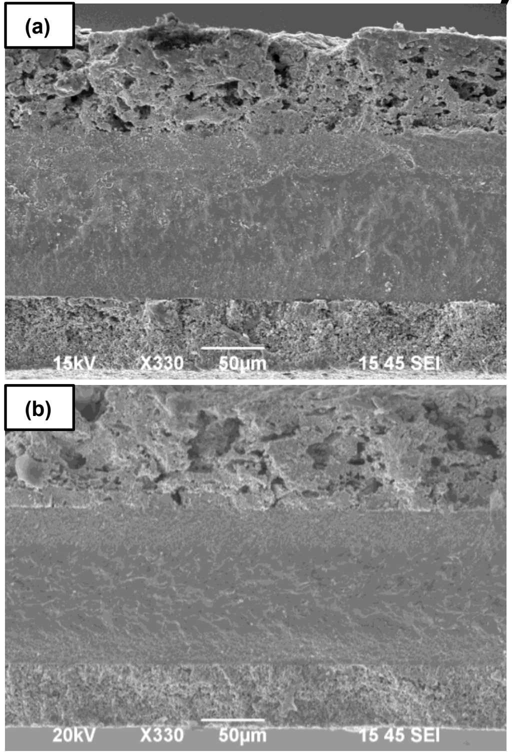

Figure 9. Cross sectional SEM image for CO_2 electrolyser cells: (a) before galvanostatic test, and (b) After galvanostatic test at 0.4 A.cm^{-2} for 48 hours.

1:3 Co-Ni alloy

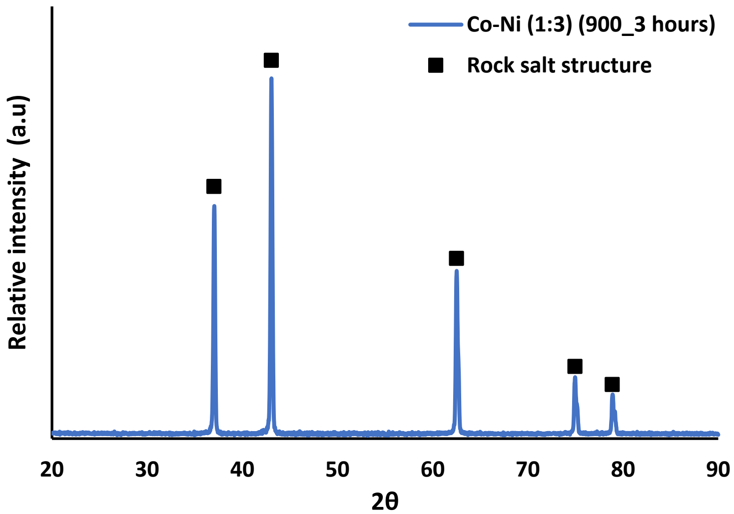

Figure 10. XRD pattern for 1:3 Co-Ni alloy calcined at 900°C for 3 hours.

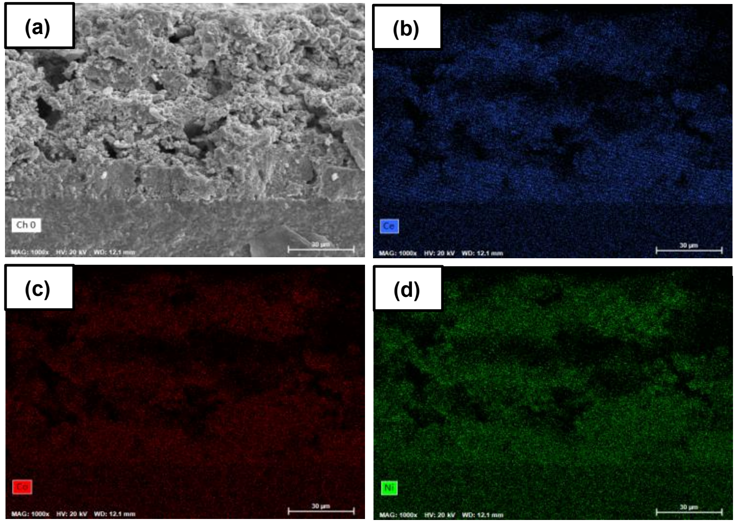

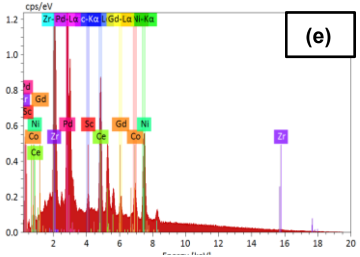

Map

Element	At. No.	Mass [%]	Mass Norm. [%]	Atom [%]	abs. error [%] (3 sigma)
Sc	21	0.99	1.08	2.26	0.12
Co	27	3.95	4.30	6.84	0.35
Ni	28	11.17	12.18	19.44	0.92
Zr	40	25.95	28.29	29.06	2.97
Pd	46	27.48	29.96	26.37	2.64
Ce	58	20.33	22.16	14.82	1.68
Gd	64	1.85	2.02	1.20	0.26
		91.72	100.00	100.00	

Figure 11. SEM image analysis for 1:3 Co-Ni infiltrated GDC scaffold: (a) cell cross section, (b) cerium distribution representing the GDC scaffold , (c) cobalt distribution throughout the scaffold, (d) Nickel distribution throughout the scaffold, and (e) elemental analysis spectrum and results.

1:3 Co-Ni Electrochemical Performance

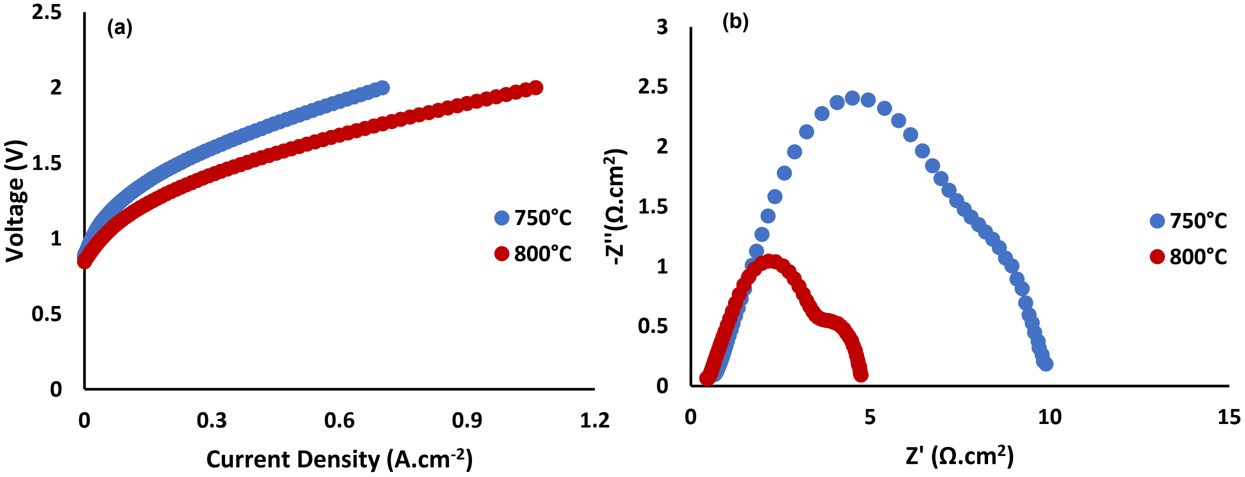

Figure 12. Performance of 1:3 Co-Ni infiltrated cathodes tested at different temperatures: (a) polarization curves and (b) Nyquist curves.

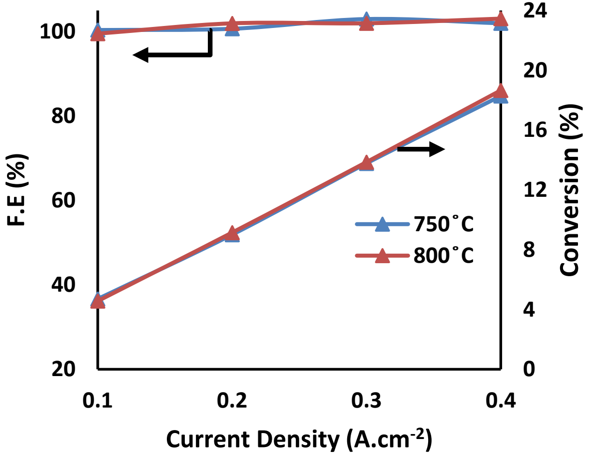

Figure 13. Faradaic efficiency and CO_2 conversion for 1:3 Co-Ni infiltrated cathodes.

Preparation of $La_{1-x}Sr_xFeO_{3-\delta}$ (LSF-X) electrocatalyst

Infiltration: introduce metal catalyst components as a solution into porous electrolyte scaffold[1,2].

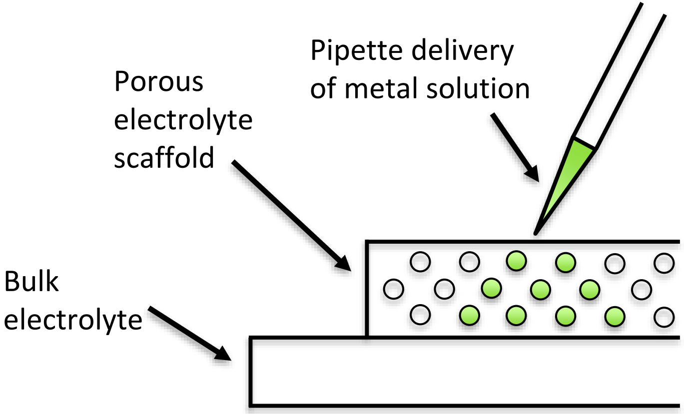

Calcination at a temperature to form appropriate electrocatalyst phase.

Verify electrocatalyst with X-ray diffraction (XRD) & scanning electron microscopy/energy dispersive spectroscopy (SEM/EDS).

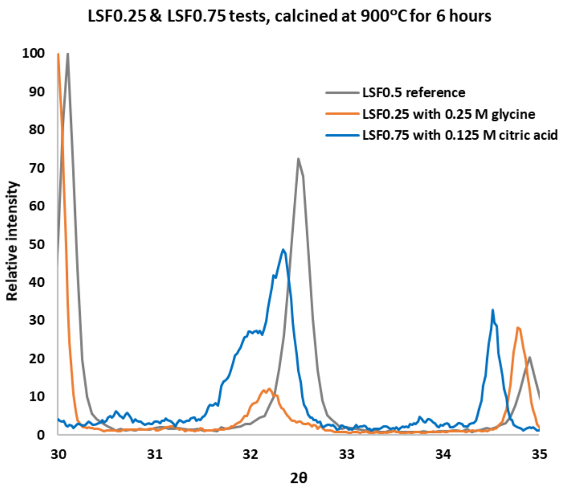

Figure 14. XRD spectra of LSF-0.25 & LSF-0.75 infiltrated cells & a LSF-0.5 reference in a perovskite-specific peak region.

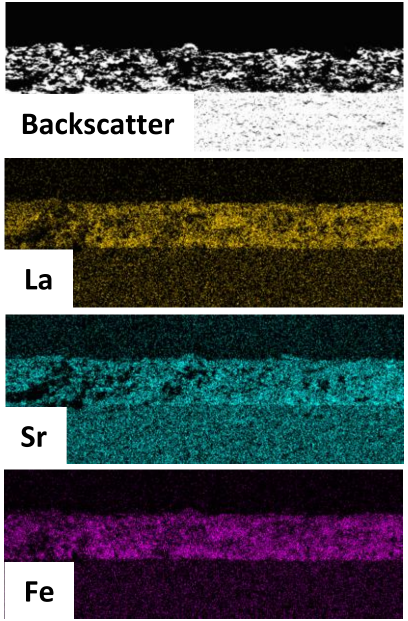

Figure 15. Cropped SEM/EDS images, showing metal content of LSF-0.25 cell.

1. Kasick et al. In *2020 AIChE Annual Meeting*; San Francisco, CA, 2020.
2. Fan et al., *J. Alloys Compd.* **2017,** *723,* 620-626.

e-ODH operation, conversion & yield trends

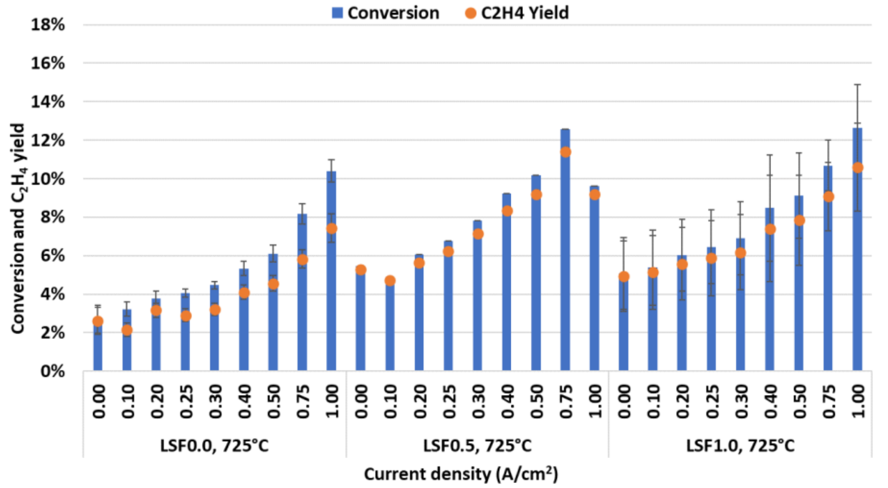

Figure 16. Effect of LSF composition at 725 °C.

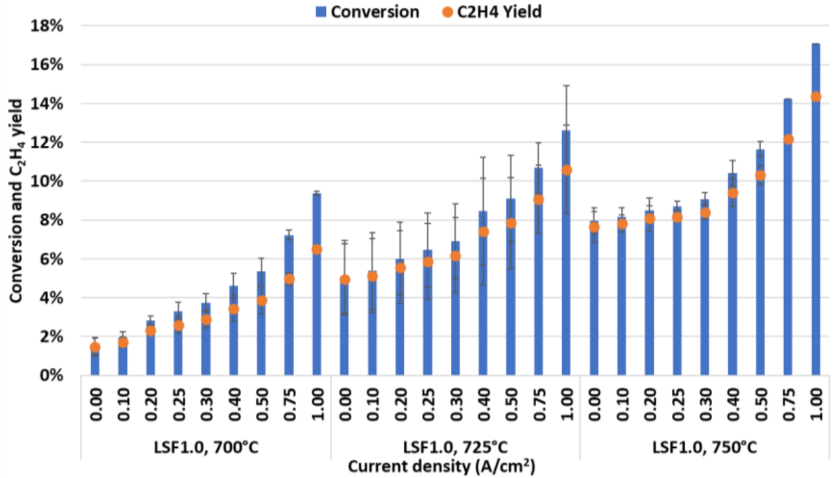

Figure 17. LSF-1.0 performance with operational temperature from 700-750 °C.

Observations:

- LSF-0.0 conversion and yield percentages were lower than higher-Sr LSF compositions & did not increase with every increase in current density.
- LSF-0.5 conversion and yield percentages were towards the upper range of those for LSF-1.0

Observations:

- Higher temperatures result in higher conversion and yield percentages, likely due to higher background thermal cracking.
- For LSF-1.0 at all three temperatures, conversion and yield increased with each current density increase.

e-ODH operation, product selectivity trends

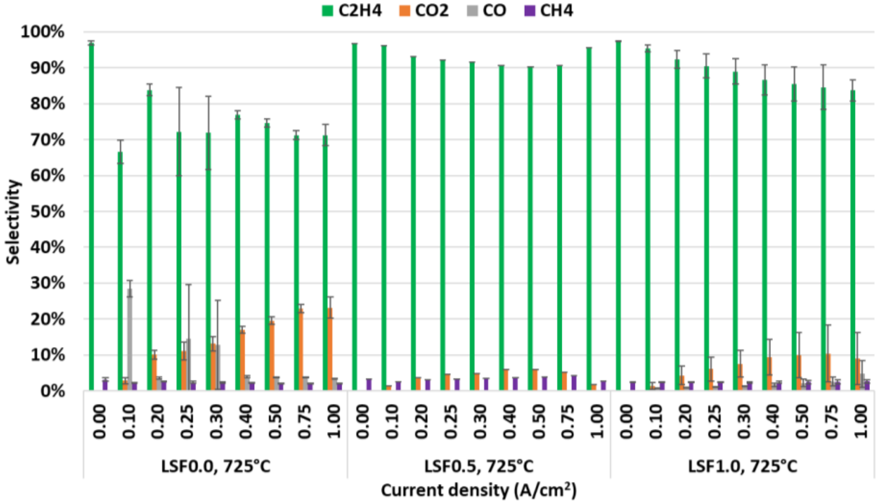

Figure 18. Effect of LSF composition on performance at 725 °C.

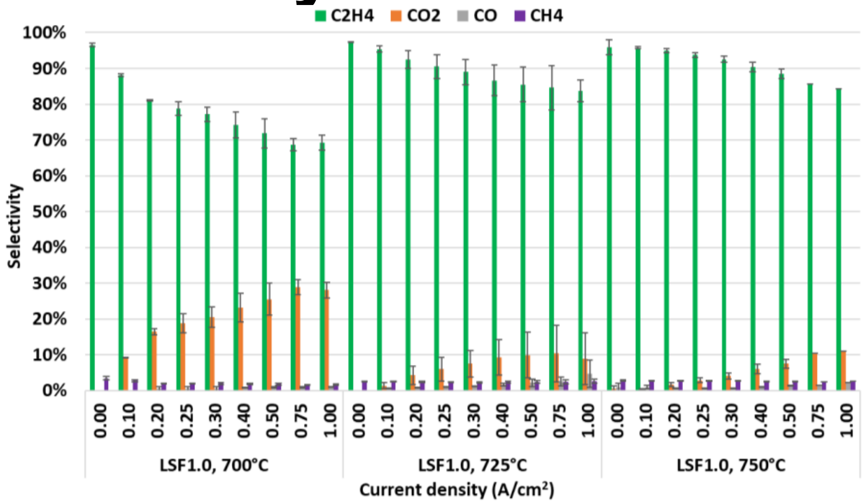

Figure 19. LSF-1.0 performance with operational temperature from 700-750°C.

Observations:

- LSF-0.5 ethylene selectivity was higher than that for LSF-0.0 and within the range for LSF-1.0.
- For all tested LSF composition, selectivity for CO_2 production tended to increase with increasing current density.

Observations:

- Across the tested temperatures, selectivity for CO_2 production tended to increase with increasing current density.
- Higher temperatures generally resulting in higher ethylene selectivities.

Summary

CO_2 electroreduction

- CO_2 electroreduction performance of transition metal catalysts (Co, Ni, Cu) evaluated from 750-850 °C
  - Infiltrated cathodes showed marked enhancement in performance compared to non-infiltrated designs
  - The electrochemical performance enhanced with temperature
  - Co and Ni infiltrated cathodes showed similar electrochemical performance likely due to their similar oxophilicity
  - Cu infiltrated cathode overpotential is higher likely due to high its greater oxophilicity
  - Co infiltrated design demonstrated stable electroreduction performance for 48 hours of operation at 850 °C
- Co-Ni infiltrated cathodes were successfully fabricated and tested for CO_2 reduction at 750-800°C
  - Fabricated cells showed uniform catalyst distribution throughout the scaffold structure
  - Co-Ni-O solid solution (rock salt structure) was the dominant phase for the Co-Ni catalyst
  - Electrochemical performance of 1:3 Co-Ni was similar to Co and Ni infiltrated cathodes

e-ODH

- Anodes infiltrated with $La_{1-x}Sr_xFeO_{3-\delta}$ (x=0 and 1) were tested from 700-750°C
  - LSF-1.0 showed higher ethane conversion and more consistent ethylene selectivity than LSF-0.0
  - For LSF-1.0, increasing temperature increased ethane conversion and ethylene selectivity
  - For LSF-0.0, ethane conversion increased with temperature.
  - For LSF-0.0, ethylene selectivity fluctuated and did not follow a particular trend with increasing temperature.
- Intermediate LSF composition (x=0.25, 0.50, and 0.75) testing at 725°C underway
  - Preliminary LSF-0.50 results indicate increasing ethane conversion and decreasing ethylene selectivity with current density.
  - Preliminary LSF-0.25 and LSF-0.75 results consistent with trends observed in LSF-0.50.
  - Additional testing underway to assess the effect of A-site substitution on e-ODH performance.

Acknowledgments

- OHIO Colleagues: Andrew Kasick, Ahmad Abu Hajer, Dr. Damilola Daramola, and Dr. Sam Velraj
- U.S. Department of Energy-National Energy Technology Laboratory via Award DE-FE0031709
- Project Manager: Dr. Naomi O’Neil

Additional Slides

Cobalt Oxidation

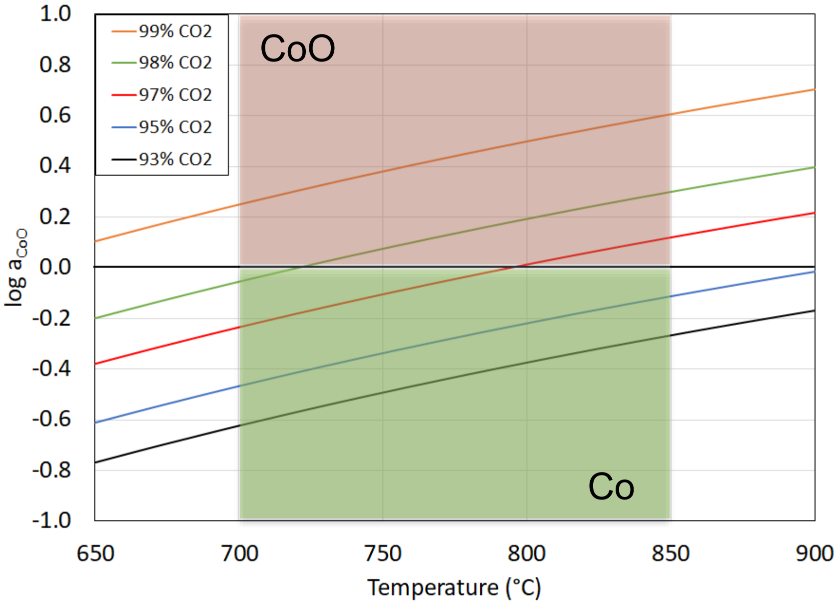

Figure 8. CoO Activity in CO_2/CO Mixtures.

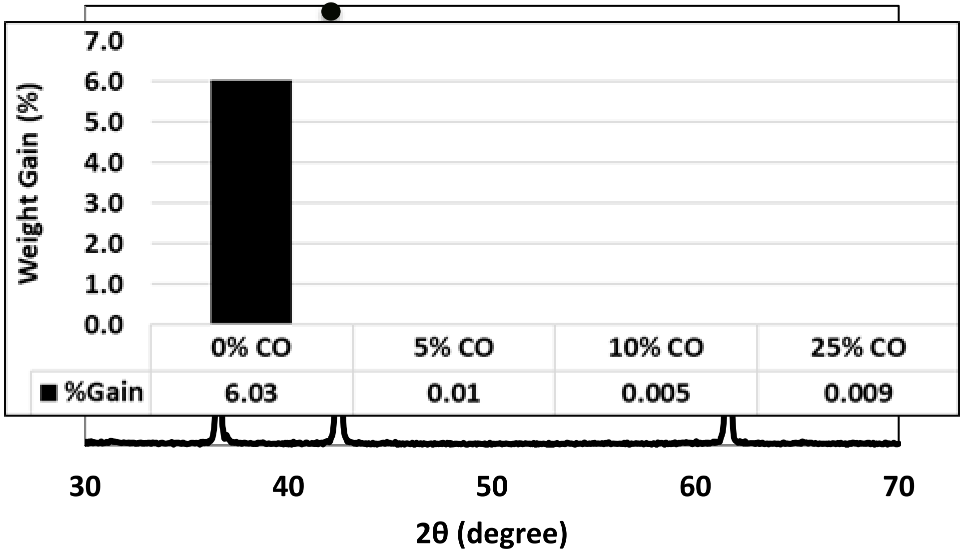

Figure 9 ... Exposure at 700 °C ... vol.% CO_2.
Exhaust Recycle

Nickel Oxidation

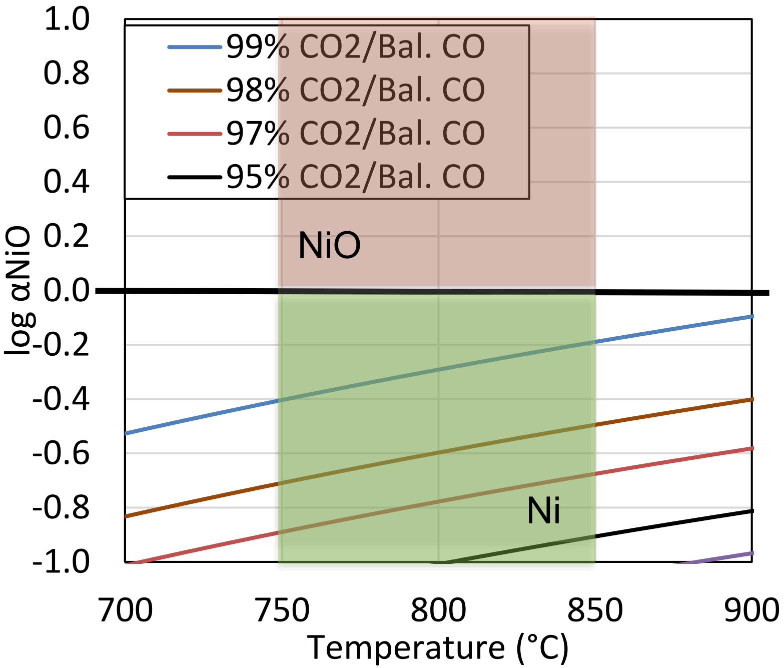

Figure 11. NiO Activity in CO_2/CO Mixtures.

- Ni/CO_2 Oxidation Reactions
  - $Ni(s) + \mathrm{CO}_{2(g)} \rightarrow NiO(s) + \mathrm{CO(g)}$
  - $a_{NiO} = K\dfrac{a_{CO_2}}{a_{CO}}$

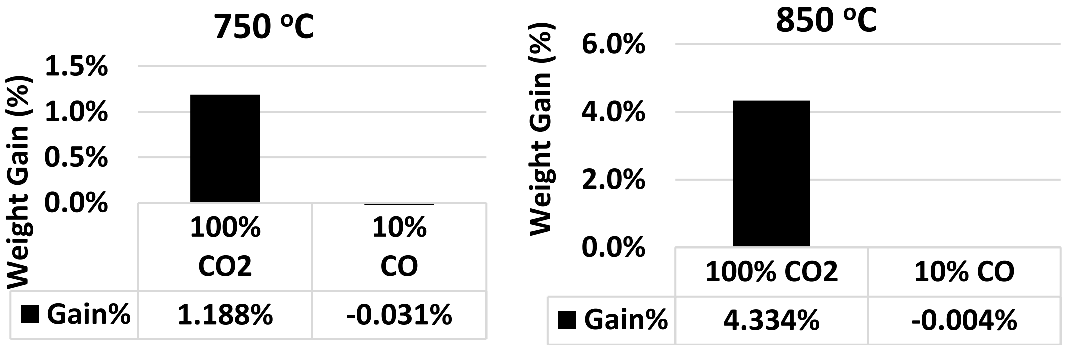

Figure 12. weight gain measured for Ni in 100%CO_2 and 10% CO addition Mixtures at 750 and 850 ºC.